ISSN 1946-7664. MCFNS 2022
Vol. 14, Issue 1, pp. 15–31
Mathematical and Computational Forestry & Natural-Resource Sciences

AVAILABLE ONLINE AT HTTP://MCFNS.COM

Submitted: Jan. 15, 2022
Accepted: Mar. 9, 2022
Published: Apr. 30, 2022
Last Correction: May 2, 2022

MISSION IMPOSSIBLE: POSITIONS DETERMINED BY BASIC MAPPING-GRADE AND RECREATION-GRADE GNSS RECEIVERS CANNOT EMULATE THE ACTUAL SPATIAL PATTERN OF TREES

T. Lee , P. Bettinger , K. Merry , V. Bektaş , C.J. Cieszewski

Warnell School of Forestry and Natural Resources, University of Georgia, Athens, GA, USA

Abstract. Global navigation satellite systems (GNSS) can provide valuable spatial information for effectively mapping and navigating through complex terrain and forest conditions. Relatively accurate positional information is essential for certain algorithms and models that base analyses on the spatial arrangement of trees, and for management of forestry operations. The accuracy of GNSS receivers has been well-tested under many environmental conditions. Depending on the technology selected and conditions within which it is employed, different amounts of variation will occur in the determination of a horizontal position. However, studies involving the spatial pattern and distribution of tree locations (point positions) observed by independent GNSS receivers generally have not considered the horizontal position error inherent in the spatial data. We conducted this study to investigate whether tree locations determined by recreation- and mapping-grade GNSS receivers can adequately represent the real point pattern of trees in a forest. The study area was a pine seed orchard located at the Whitehall Forest in Athens, Georgia (USA), that consisted of a regular pattern of trees. We tested three different GNSS receivers: one mapping-grade receiver and two recreation-grade receivers (traditional, handheld-type, and non-traditional types, GPS watch). With each receiver we determined tree locations at cardinal points around the stems of 112 trees (at North, South, East, and West, sides of the stems) and estimated the middle point measurement of two cardinal points (North-South and East-West). In addition, we used the average of all cardinal points (All) to determine tree locations. We compared these observed tree locations to actual tree locations, which were determined through precise field measurements and high-precision GPS base points. This study confirmed that the horizontal positional error of mapping grade receivers was significantly lower than those of recreation grade receivers, regardless of measurement method. However, the observed point pattern of trees from the GNSS observations of both recreation- and mapping-grade receivers failed to adequately represent the actual regular point pattern of the trees, as the positional error observed was not consistently projected in the same direction and with the same magnitude.

Keywords: Global navigation satellite system, complete spatial randomness, regular pattern, clustered pattern, root mean squared error, GPS receivers.

1 Introduction

The natural pattern of the location of trees is a result of ecological processes involving self-thinning and competition between trees and seed dispersal mechanisms. In planted forests, the pattern of the location of trees is operationally influenced yet can also be influenced by ecological processes involving pioneer and natural establishment of non-planted trees. For assessing patterns of trees, spatial point pattern analysis (SPPA) has become increasingly popular in ecological research (Gadow et al. 2012, Velázquez et al. 2016, Woodall 2002, Wiegand et al. 2013, Wiegand & Moloney 2013). As a way for analyzing the pattern of trees, SPPA allows one to characterize forest structure (i.e., dispersed, random, clustered) and test ecological hypotheses about underlying natural processes (Law et al. 2009, Ripley 1981, Velázquez et al. 2016, Wiegand & Moloney 2013). For example, SPPA has been used to investigate the effects of seed dispersal mechanisms (Garzon-Lopez et al. 2014,

Seidler & Plotkin 2006) and to analyze the role of interactions and competition between trees (Dohn et al. 2017, Fajardo et al. 2006, Uria-Diez & Pommerening 2017).

SPPA compares the pattern of observed spatial data to a null model using various summary statistics. To evaluate the pattern of objects, SPPA uses point locations (i.e., locations trees, nests, or shrubs) and supplementary information (attributes) that characterize the object (i.e., surviving versus dead, species, size) (Velázquez et al. 2016). Further, the data can be classified as unmarked and marked spatial data based on its properties. For example, unmarked spatial data having *a priori* properties include such things as tree species, while marked spatial data having *a posteriori* properties including such things as status (surviving versus dead), size, or some other property from a marking process (Velázquez et al. 2016, Wiegand & Moloney 2013). SPPA provides a description of the spatial pattern of measured features using summary statistics, which are classified as either (a) numerical or functional or (b) location- or point-related (Illian et al. 2008, Wiegand & Moloney 2013). Outcomes of SPPA can represent spatial pattern as a value (e.g., intensity or the mean distance to the nearest neighbor) (Pommerening & Grabarnik 2019, Velázquez et al. 2016), and these have been widely used in modern point pattern analysis to represent a point pattern as a function of scale (Wiegand & Moloney 2013).

The null model (also referred to as the point process model or point process) associated with a SPPA analysis is a mathematical model representative of a certain point pattern (Wiegand & Moloney 2013). The null model plays an important role in SPPA because it is used to determine whether an observed spatial pattern can be statistically distinguished from it or not (Carrer et al. 2018, Diggle 2013, Wiegand & Moloney 2013). The simplest version of a null model is complete spatial randomness (CSR) following the homogeneous Poisson process, which assumes an equal intensity or distribution of objects across a study area (Carrer et al. 2018, Law et al. 2009, Wiegand & Moloney 2013). One might expect that a naturally regenerated or uneven-aged forest would possess CSR with respect to tree locations. Otherwise, a null model may also follow a heterogeneous Poisson process, which has a different intensity function that depends on the locations of objects within the study area (Carrer et al. 2018, Pommerening & Grabarnik 2019, Wiegand & Moloney 2013). SPPA compares an observed pattern to a confidence envelope, or group of null models generated by Monte Carlo simulation (Law et al. 2009). When an observed pattern of objects lies outside of a confidence envelope with a certain confidence level, this provides evidence of a departure from the null model (Wiegand & Moloney 2013). Otherwise, when an observed pattern of objects fails to prove departure from the null models, this indicates that there is no correlation between observed points, which is equivalent to saying that there are no ecological interactions evident in the data (Pommerening & Grabarnik 2019).

The result of SPPA is influenced by many factors. For example, spatial scale (size of sampling site) for the detection of tree patterns can be important, as larger sampling scales allow one to better detect a spatial pattern, such as clustering, that are not evident at smaller scales (Carrer et al. 2018, Garzon-Lopez et al. 2014). Further, using the heterogeneous Poisson model as a null model for emulating CSR may provide more reliable results than using the homogeneous Poisson model, since constant intensity across a study site may not be guaranteed (Carrer et al. 2018). Perry et al. (2006) and Hui et al. (2007) suggested that each summary statistic used in evaluating spatial pattern has limitations and strengths. Further, Gadow et al. (2012) and Pommerening (2008) pointed out that the application of spatial pattern analysis may be limited by the size of study area. Therefore, Velázquez et al. (2016) and Wiegand et al. (2013) suggested that the various summary statistics should be applied together, to avoid omitting important meanings from spatial patterns.

In describing the distribution of trees in a forest, the positions (spatial coordinates) of tree boles are an essential input for SPPA (Aguirre et al. 2003, Pommerening 2002). For forest growth and yield purposes, the positions of tree boles are also needed for distance-dependent tree growth models. However, collecting spatial data of tree bole positions can be very challenging due to the cost and time associated with the data collection effort, making the practical application of SPPA challenging (Aquirre et al. 2003, Gadow & Hui 2002, Gadow et al. 2012, Velázquez et al. 2016). For example, it might take more than 30 minutes to determine a tree's location if a survey-grade GNSS receiver is used. This is one reason why survey-grade GNSS receivers are not widely used in practice except to locate property corners or other important landscape positions. Further complicating the collection of tree bole locations, several studies that have been conducted to evaluate GNSS receiver accuracy in forested areas revealed that mapping-grade and recreation-grade GNSS receivers have horizontal positional errors ranging on average more than 2m (Danskin et al. 2009, Ransom et al. 2010, Sigrist et al. 1999) and more than 6m (Danskin et al. 2009, Lee et al. 2020), respectively, in any direction from the true position. A greater positional error is often observed when using recreation-grade GNSS receivers (small inexpensive GNSS specific units, cellular phones, watches, etc.), yet recreation-grade receivers are still utilized frequently due to their applicability and accessibility. Accord-

ing to Bettinger et al. (2019), foresters in the southern United States commonly use cellular phones and tablets (70.6%) for positioning and navigation, followed by other recreation-grade receivers (49.4%) and mapping-grade receivers (43.8%). Bettinger et al. (2019) also indicated that only a few respondents used survey-grade receivers (2.8%) and mapping-grade receivers with differential processes (DGPS) (15%) in their normal work activities. Platforms such as iNaturalist and iTree Eco have also allowed citizen observers to provide positional data using recreation-grade GNSS receivers (Fauzi et al. 2016a). Therefore, the quality of positions determined by GNSS for individual trees may be a great concern.

Compounding the issue of horizontal position accuracy, the physical direction of the position error is often unreported and assumed randomly distributed around a true position, yet the directionality of error may be influenced by nearby vegetation (Bettinger & Merry 2012b). Current SPPA studies do not consider the inherent error in positions determined by GNSS receivers, potentially leading to analysis error when spatial relationships are based on the distance between objects (i.e., distances between objects or counts of objects within certain distance). To overcome these challenges, different approaches to estimate the positions of trees have been explored, including the use of base maps facilitated by satellite images (Atkinson et al. 2007, Moustakas et al. 2008), aerial images from aircraft or unmanned vehicles (Garzon-Lopez et al. 2014, Moustakas et al. 2008, Xu et al. 2019), or LiDAR (light detection and ranging) including terrestrial and airborne laser scanning (Trochta et al. 2013). However, there are limitations in estimating the location of tree stems from these types of images, due to image quality, spatial resolution, and feature displacement. Specifically, when identifying the location of a tree bole, an interpreter is more commonly locating the centroid of a tree canopy as opposed to the location of a tree bole, and the corresponding pattern concerning centroids of tree crowns may differ from the pattern concerning the tree boles (Uria-Diez & Pommerening 2017, Vacchiano et al. 2011). Further, the crowns of some overtopped or suppressed trees may not be evident in an analysis of satellite or aerial imagery. Additionally, the quality of images generated by LiDAR can be significantly deteriorated by weather conditions (water, dust, or wind) and the presence of rough terrain (Trochta et al. 2013).

Tree bole coordinates have been used in various studies to assess spatial pattern (Dohn et al. 2017, Hui et al. 2007, Law et al. 2009, Uria-Diez & Pommerening 2017), but the specific methods employed for collecting the coordinates of tree bole locations are often not described or it is suggested that the locations were determined using GNSS technology. Therefore, our objectives for this study are twofold. First, we evaluate the inherent positional error of tree bole locations using three different types of GNSS receivers and several assumptions regarding the data collection protocols. These data collection protocols emulate common practices employed by the typical forestry professional in the southern United States for capturing the position of resources of interest. Therefore, survey-grade GNSS receivers and the use of real-time kinematic (RTK) positioning were not tested. In RTK positioning, the mobile unit (the one used by the professional collecting data) relies on the acquisition and use of real-time position correction information that is supplied by an independent reference station (or base station) or a virtual reference station positioned over a known location. Second, we compare the observed spatial patterns of tree boles to the actual spatial pattern of trees measured using ground surveying methods, to determine whether tree bole coordinate positions determined from GNSS receivers can retain the fidelity of the real-world spatial pattern of trees.

2 Materials and Methods

This study was conducted in a loblolly pine (*Pinus taeda*) seed orchard within the Whitehall Forest in Athens, GA. Trees were planted in a regular grid arrangement, with an average spacing of about 6.15m. At the time of this study, the trees were 34 years old (Figure 1). While representative of a regular pattern, the distances between the trees along and between rows are not exact, due to the natural growth and development forces on the trees. The density of the seed orchard was estimated to be 193 trees ha^{-1}, with a basal area of 26.4 m^2 ha^{-1}. It is uncommon to use a seed orchard as study site for SPPA because the distribution (pattern) of trees is uniformly dispersed. However, by using the seed orchard we were able to avoid influence associated with the spatial placement of plots having environmental heterogeneity and potential clustering characteristics (Garzon-Lopez et al. 2014). A total 112 trees were used across the study site (0.61 hectare), which is generally comparable to area required to reliably assess spatial pattern (Carrer et al. 2018). Therefore, this study site serves as a control pattern for evaluating the point pattern of tree bole positions determined using GNSS technology.

To determine the spatial locations of tree boles in the study area, three different GNSS receivers were used: a Trimble GNSS receiver (Juno T41, Trimble Inc., USA), a Garmin GNSS receiver (Oregon 700, Garmin, Olathe, KS, USA), and a Suunto GPS watch (Ambit Peak 3, Suunto, Finland). The Trimble Juno T41 GNSS receiver is classified as a mapping-grade receiver based on an estimated horizontal accuracy of 1 to 5m (Lee et al. 2020)

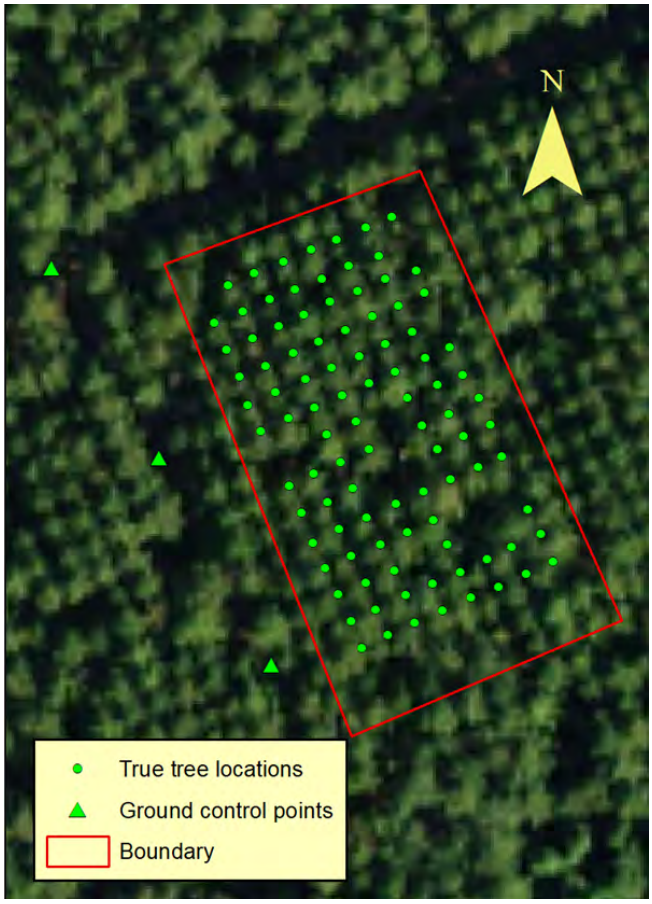

Figure 1: The study plot with 26 control points. These control points were determined based on the surveyed control points (#7, #20, CP1, and CP2) using trilateration. Each control points apart from each other in 6 meters.

and a general price range of $1,000 to $9,000 (Bettinger & Merry 2011). The Garmin Oregon 700 GNSS receiver and the Suunto GPS watch are classified as recreation-grade receivers based on an estimated horizontal accuracy between 6 to 12m (Danskin et al. 2009, Lee et al. 2020) and a general price range of $100 to $700. These horizontal accuracy statements are based on common, practical use of the devices, which consist of an average of a collection of position fixes (all determined within about 30 seconds or less) from the mapping-grade device, and one waypoint from the recreation-grade devices to determine a horizontal position.

The Trimble GNSS receiver was equipped with a relatively large GPS antenna manufactured by Inpaq technology Co. Ltd (Taiwan) (70×43.18×9mm), which has the ability to utilize both GPS (United States) and GLONASS (Russian Federation) commercially available satellite signals. The receiver uses SOLO Forest software (Trimble Inc., USA) to facilitate data collection with masks limiting the maximum PDOP (positional dilution of precision) and minimum SNR (signal to noise ratio), and allowing the use of the Wide Area Augmentation System (WAAS) for near-real time signal augmentation. The maximum PDOP and minimum SNR values were set to 8 and 4, respectively, and WAAS augmentation was enabled. A PDOP value reflects the quality of satellite constellation arrangement; a lower PDOP value suggests a preferable satellite geometry (wider satellite spacing), which can help to minimize trilateration error and perhaps provide more accurate position descriptions (Lewis et al. 2007). A PDOP value of 4 or less suggests rather good satellite geometry has been obtained, and a PDOP value greater than 9 suggests rather poor satellite geometry. So, the maximum PDOP value of 8 assumed represents a moderate setting for satellite geometric arrangement in this study. A position was determined by the Trimble receiver by averaging around 15 position fixes (one per second) during each visit to each tree, which is typical in practice when using this device.

The Garmin GNSS receiver was equipped with a GPS antenna made by Cirocomm Technology Corp. (Taiwan) (size: 15×15×4mm). Like the Trimble receiver, the Garmin receiver can utilize both GPS and GLONASS satellite signals. The Garmin receiver has limited configuration options and does not allow one to set the maximum PDOP and minimum SNR values. However, the WAAS augmentation system was employed. The Garmin receiver has a function to determine a position by averaging multiple position fixes, but this function was not used in this study. Positions were determined using a single position fix (waypoint), which is common in practice when using this device. Data was collected and stored using the WGS84 coordinate system, and data were downloaded using “basecamp” software (Garmin International, USA).

The Suunto GPS watch is considered a non-traditional recreation-grade receiver. It is equipped with a GPS antenna equal in size to the Garmin GNSS receiver’s (size: 15 x 15 x 4mm) made by Patron Co. Ltd (Korea). Similar to the Garmin receiver, the Suunto GPS watch has limited configuration options. A user can only change the GPS coordinate system specified for data collection. Here, the GPS coordinate system for data collection was set to UTM NAD1983. The Suunto GPS watch has no function for averaging multiple position fixes to determine a location, so a position was recorded as one point per each visit to each tree. Prior analysis of this GPS watch (Lee et al. 2020) suggested that it can provide an average horizontal position accuracy of 29.6m in an uneven-aged deciduous forest during the leaf-on conditions, and 22.1m in an older pine forest in the southern United States.

In prior observational studies, average horizontal position accuracy has been estimated for various types of GPS devices in forested conditions. However, the direction of the error around a control point was not assessed except in one study (Bettinger & Merry 2012b). The combination of horizontal and directional error could affect the pattern of individual trees if mapping them were the main purpose. This interplay has yet to be researched and represents an area of novelty of this study. If one assumed that the direction of error of point locations for features such as trees was consistent within a short period of time, then the determined point positions should represent well the point pattern of the trees that they represent. Unaugmented GNSS position fixes collected with autonomous recreation-grade GNSS receivers have been used to develop databases of urban tree locations (Green et al. 2016, Tait et al. 2009) and rural forest tree locations (Fauzi et al. 2016b), yet in the latter case the data were deemed unsuitable for adequately describing individual tree locations. Alternative technologies such as RTK GNSS (Khot et al. 2006), differential GNSS, or simultaneous localization and mapping (SLAM) algorithms (Fan et al. 2018) may help improve horizontal position accuracy for individual trees in forests. However, as we noted earlier, we did not employ these augmentations during our tests as they are not commonly used in practice in the southern United States (Bettinger et al. 2019).

The basis for the real point pattern of tree boles in our study area involved a ground survey of tree locations, beginning with the determination of three ground control points using a mapping-grade receiver (Nomad 1050, Trimble Inc., USA) equipped with an external antenna (Garmin GPS 19x HVS, Garmin International, USA) and situated on a road next to the seed orchard (Figure 1). The mapping-grade receiver was allowed to warm up for 30 minutes, then position fixes were collected for a 20-minute time period on three different occasions. The mean northing and easting for each measurement period was then used to estimate each control point location. The mean northing and easting coordinates had standard deviations of 0.17m and 0.45m, so these ground control points were considered to be relatively accurate locations. Tree bole locations were then estimated by triangulating the physical distance between trees, the distance from a control point, the azimuth from each tree to a ground control point, and the azimuth from tree to tree (Kiser 2008). These measurements were collected using a measuring tape and a laser rangefinder (TruPulse 360R, Laser Technology Inc., Centennial, CO, USA). The diameter at breast height (DBH) for each tree was also measured. In estimating the distance between two trees or between trees and the ground control point, the distance to the center of a tree stem was determined by adding half of the DBH to the measured distance. As multiple distance measurements were collected between sample trees, tree location was estimated with the optimization function using R (version 1.1.463, RStudio, Inc., Boston, MA, USA) to minimize the error derived from the difference between measured distance and calculated distance. Since the laser rangefinder has a manufacturer's reported error of less than 0.5˚in azimuth, the manufacturer's angle error was considered by generating random numbers within this error range (0˚ to 0.5˚) centered on the measured angle value to obtain the calculated distance. The estimated tree locations by optimization were assumed to be the basis for comparison against the GNSS-determined tree locations.

Tree bole locations determined using the three GNSS receivers were collected on four different occasions, at each cardinal position (north, south, east, and west) around a tree, and averaged to investigate whether the data collecting location around trees had significant effects on positional accuracy. In total, there were seven different data collection methods:

Method "All": the mean position of 16 points collected from every cardinal direction

Method "NS": the mean position of 8 points collected from north and south sides of each tree

Method "EW": the mean position of 8 points collected from east and west sides of each tree

Method "N": the mean position of 4 points collected from north side of each tree

Method "S": the mean position of 4 points collected from south side of each tree

Method "E": the mean position of 4 points collected from east side of each tree

Method "W": the mean position of 4 points collected from west side of each tree

The data collection process was time consuming and therefore it was not possible to complete in a single day. Instead, data were collected over a period of three weeks. We visited the study site at a similar time period (between 1 p.m. and 4 p.m.) of the day only when the weather was not severe (rainy, cloudy or windy). In this study, however, the weather conditions were not monitored, as it has been shown that local climatic conditions have little effect on positional accuracy of mapping-grade and recreation-grade GNSS receivers (Bettinger & Fei 2010, Ransom et al. 2010, Merry & Bettinger 2019). During the data collection effort, GNSS receivers were held on top of a monopod with a leveling device, to maintain a constant position. The monopod was located 1m away from the stem of each tree, and the researcher always stood on the north side of the monopod. One half of each tree's DBH was added to the 1m of distance between the tree and the position of the monopod. This

distance was used to locate the center of the tree stem from observed spatial data. Before collecting coordinate locations, both the Garmin GNSS receiver and the Trimble GNSS receivers were allowed to warm up for about 5 minutes. The Suunto GPS watch did not need warm-up time because it was always on and ready for collecting spatial data.

The first hypothesis of the study was that the horizontal positions determined using the different GNSS devices and the different methods to estimate tree bole location were not statistically different. The horizontal accuracy of data collected using each GNSS receiver was determined using the root mean square error (RMSE), which can be calculate as

$$RMSE = \sqrt{\frac{\sum_{i}^{n}\left((x_i - x)^2 + (y_i - y)^2\right)}{n}} \quad (1)$$

Where n is the total number of observations in a visit; i is the ith observation of the visit; x_i and y_i are the longitude and latitude, respectively, of the ith observations; and x and y are the assumed true easting and northing of the associated tree location. The RMSE is widely used for horizontal position accuracy with GNSS data (Ransom et al. 2010, Sigrist et al. 1999). In addition to it, the root squared error of the mean (RSEM) was calculated based on the mean center's coordinates. The direction and tendency in collected data was investigated using a standard deviational ellipse described by an orientation angle and an anisotropic ratio (I_a) (Lee et al. 2020, Hung et al. 2019). To test the first hypothesis related to the RMSE and parameters of standard deviational ellipses, we applied the one-way ANOVA and Kruskal-Wallis test using R Studio software (2022.02.0, RStudio, Inc., Boston, MA, USA). The RSEM and parameters of standard deviational ellipses were calculated with ArcMap GIS software (version 10.7.1, Esri Inc., Redlands, CA, USA).

$$I_a = \left(\frac{R - r}{R}\right) 100 \quad (2)$$

The second hypothesis of this study was that the spatial pattern of tree locations determined using the GNSS receivers was completely random. The seed orchard trees planted in a regular pattern allowed us to assess this hypothesis that GNSS-determined positions are representative of a certain spatial pattern. To analyze the observed distributions (patterns) of tree boles, various kinds of distance-based statistical methods were applied including the average nearest neighbor (ANN) analysis, $g(r)$ function, and $\hat{L}(r)$ function so not to omit important information regarding spatial scale (Velázquez et al. 2016, Wiegand et al. 2013). The ANN analysis was applied using ArcMap GIS software (version 10.7.1 Esri Inc., Redlands, Cam USA) to determine whether the observed pattern of tree distribution in the seed orchard follows the CSR process. ANN analysis provides the ANN ratio (or an *R-statistic*) by comparing the average distance ($\bar{D}_0$) from each object (i.e., tree position determined using a GNSS receiver) to its nearest object (i.e., another tree position) against the expected average distance ($\bar{D}_E$) under CSR. It also provides its significance using $p-$values and z-score indicating whether the observed patterns are statistically departed from the null model of CSR (Wiegand & Moloney 2013) as follows:

$$\bar{D}_0 = \frac{\sum_{i=1}^{n} d_i}{n} \quad and \quad \bar{D}_E = \frac{0.5}{\sqrt{n/A}} \quad (3)$$

$$ANN = \frac{\bar{D}_0}{\bar{D}_E} \quad (4)$$

Where d_i is the distance between tree i and its nearest neighboring tree, n is the total number of trees, and A is the study site area.

In this study, the ANN ratio (R) represents how the point patterns of the GNSS-determined positions are distributed. For example, when $R = 1$, points are considered to be distributed randomly. When $R > 1$, points exhibit a dispersed point pattern (which would most closely emulate a regular pattern). When $R < 1$, points are considered to exhibit a clustered pattern (Clark & Evans 1954).

The $L(r)$ function is a transformed version of 'Ripley's K function ($K(r)$)' and is widely used for SPPA in ecological literature (Gadow et al. 2012, Law et al. 2009, Wiegand & Moloney 2013). The $K(r)$ function describes the pattern based on the quantity of the intensity (λ) and $K(r)$, $\lambda \cdot K(r)$, which is the expected number of further points within distance r of the typical point (Wiegand et al. 2013, Wiegand & Moloney 2013). Since the expected number of points is increased at the rate of r^2 when using the $K(r)$ function, it can be transformed to the $L(r)$ function (Wiegand & Moloney 2013). Calculated from $K(r)$, the $L(r)$ function (Besag 1977) is derived as follows:

$$K(r) = \frac{A}{n^2} \sum\nolimits_{i=1}^{n} \sum\nolimits_{j}^{n} w_{ij}^{-1} I_r(u_{ij}) \quad (5)$$

$$L(r) = \sqrt{\frac{K(r)}{\pi}} \quad (6)$$

Further, the $L(r)$ function can be normalized as below:

$$\hat{L}(r) = L(\mathrm{r}) - r \quad (7)$$

Where A is the study area, r is the radius, n is the number of individuals, $I_r(u_{ij})$ is an indicator function (which is either 1 when $u_{ij} < r$ or 0 when $u_{ij} > r$), and

w_{ij} is a weight value for Ripley edge correction. In this study, the $\hat{L}(r)$ function was applied because it provides more interpretable graphs than $K(r)$ and $L(r)$ (Gadow et al. 2012). Since $\hat{L}(r)$ has a value of 0 under CSR, it is easier to be assessed against the observed pattern (Wiegand & Moloney 2013). A positive value at distance r indicates that there are more points than the expected number of points, indicating a tendency toward clustering. Otherwise, a negative value at distance r means that there are less points than expected, indicating a tendency toward dispersing.

The pair correlation ($g(r)$ function) was also applied to analyze the observed patterns. The $g(r)$ function is closely related to the $K(r)$ function because both are second-order statistics. However, the $g(r)$ function is discernable in that it is a non-cumulative function, accounting the expected point density within a ring with radius (r) and width (dr) centered in the typical point (Wiegand et al. 2013). Although cumulative functions including $K(r)$ and $L(r)$ function were still frequently used, we applied the $g(r)$ function because it provides better assessments when it is compared to cumulative functions (Gadow et al. 2012, Hui et al. 2007, Law et al. 2009). When it comes to the cumulative function, effects observed at short spatial scales can obscure the effects observed at larger spatial scales (Wiegand & Moloney 2013). The $g(r)$ can be calculated from $K(r)$ (Stoyan & Stoyan 1996):

$$g(r) = \frac{dK(r)}{dr} \Big/ 2\pi r \tag{8}$$

The $g(r)$ provides value of about 1 when the data represent a CSR pattern, which is relevant to the independent of the intensity of the pattern (Gadow et al. 2012). Therefore, $g(r)$ is considered as a summary statistic that discerns whether the observed pattern is clustered or dispersed (Wiegand & Moloney 2013). For example, if the pattern has a tendency toward dispersion, it will have fewer nearby points at small distance than the expectation under CSR, so it will result in a value less than 1. Otherwise, when the pattern has a tendency toward clustering, it will have more nearby points, which is equivalent to a value larger than 1. These summary statistics are frequently used for SPPA in ecology (Hui et al. 2007, Perry et al. 2006, Velázquez et al. 2016, Wiegand & Moloney 2013). They count the number of points at or within neighborhoods of other features based on the information of inter-point distances to derive spatial information (Gadow et al. 2012, Velázquez et al. 2016).

Monte Carlo simulation was conducted for summary statistics ($g(r)$, $K(r)$, and $\hat{L}(r)$) to produce pseudo-significance levels via repeated randomization. A significant departure from the null hypothesis of CSR was estimated by 200 Monte Carlo simulations and the highest and lowest values of these simulations represent approximately 95% upper and lower confidence limits of the null model of CSR. Two hundred simulations were considered sufficient to generate envelopes for determining whether the null model can be rejected or not (Velázquez et al. 2016). The Ripley edge correction was utilized in SPPA for this study and we conducted SPPA using the "spatstat" package in R, which is a standard toolbox for this subject area (Law et al. 2009).

3 Results and Discussion

With respect to the first hypothesis of this study, the horizontal positional accuracy was analyzed for different tree bole position measurement methods and GNSS receiver types. For the Garmin receiver, occasionally it provided a sub-meter accurate horizontal position, but on average, horizontal position accuracy (as reported using RMSE) for representing the locations of trees was 10–12m (Table 1). The greatest positional error measured was 28m, and the coefficient of variation was 25–40%. For the Suunto receiver, occasionally it provided about 1m accurate horizontal positions, but on average, horizontal position accuracy was 9–13m, which was consistent with a previous study (Lee et al. 2020). The greatest positional error was 82m, and the coefficient of variation was 40–90%, suggesting much more variation in determined positions than when the Garmin device was used. For the Trimble receiver, a few sub-meter accurate horizontal positions were determined, but on average, horizontal position accuracy was 5–8m. The greatest measured positional error was 19m, and the coefficient of variation was 30–60%. Therefore, as expected, the mapping-grade receiver provided the most accurate estimates of tree positions with the lowest amount of variation compared the recreation-grade receivers. These findings were statistically significant, with p-values of less than 0.05 (Figure 2).

Regarding measurement methods that might improve horizontal positional accuracy, it was expected that determining a tree bole position using multiple cardinal positions would provide better horizontal positional accuracy regardless of GNSS receiver used. Interestingly, however, the highest and lowest mean RMSE values were observed when a tree bole position was determined at a single cardinal point regardless of GNSS receiver (Figure 3). When tree bole positions were determined from the East or North sides of a tree, the lowest positional error was observed. Otherwise, the highest positional errors were observed when tree boles were located South or West of each measurement point. Regarding the positional errors obtained by the average from all cardinal points and the average from two cardinal points (North

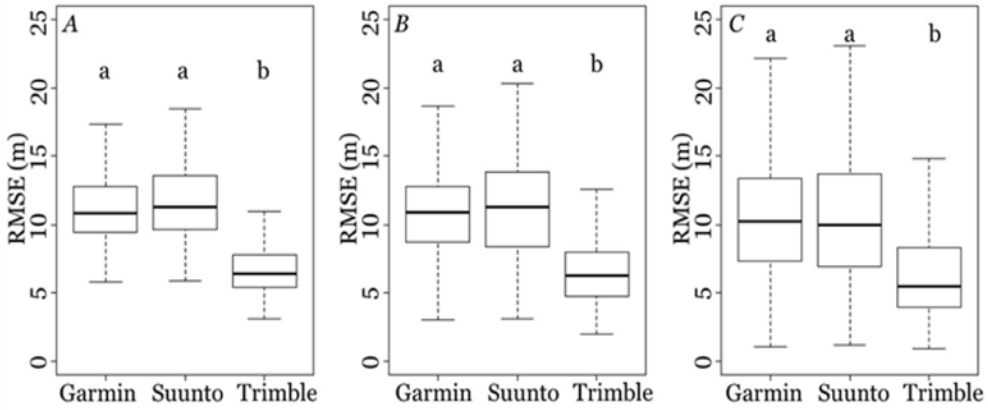

Figure 2: Boxplots for horizontal positional accuracy (RMSE) by methods and GNSS receiver types (A mean center of observed points at every cardinal point: A; A mean center of observed points at two cardinal points: B; A mean center of observed points at each cardinal point: C). *Different letters* indicate significant differences between the groups (p-value <0.05).

Table 1: A summary of raw data observations for different GNSS receiver types and measurement methods.

Device / metrics	Measurement Methods								
Garmin Oregon 700	All	Two	NS	EW	Single	N	S	E	W
Mean RMSE (m)	11.31	11.17	11.11	11.22	10.77	9.61	11.81	9.24	12.40
Min. RMSE (m)	5.92	3.11	5.47	3.11	0.97	1.71	0.97	1.41	2.74
Max. RMSE (m)	19.84	21.55	18.52	21.55	27.63	20.16	24.85	20.69	27.63
SD of RMSE (m)	2.93	3.44	3.04	3.81	4.54	3.97	4.26	3.89	5.16
n	97	194	97	97	388	97	97	97	97
Suunto watch GPS	All	Two	NS	EW	Single	N	S	E	W
Mean RMSE (m)	12.34	11.91	12.03	11.79	11.22	9.04	13.52	10.97	11.34
Min. RMSE (m)	5.96	3.15	3.27	3.15	1.06	1.06	3.67	1.34	2.53
Max. RMSE (m)	44.04	58.85	42.08	58.85	82.31	40.79	59.20	82.31	30.95
SD of RMSE (m)	5.12	6.05	4.99	6.98	7.26	5.27	6.90	10.02	5.13
n	97	194	97	97	388	97	97	97	97
Trimble Juno T41	All	Two	NS	EW	Single	N	S	E	W
Mean RMSE (m)	6.87	6.71	6.41	7.00	6.36	5.21	6.95	5.22	8.04
Min. RMSE (m)	3.14	1.95	1.95	2.02	0.91	1.12	0.91	0.92	2.97
Max. RMSE (m)	12.77	16.11	14.80	16.11	18.86	18.86	17.59	14.89	17.25
SD of RMSE (m)	2.00	2.51	2.67	2.31	3.29	3.02	3.47	2.82	2.97
n	97	194	97	97	388	97	97	97	97

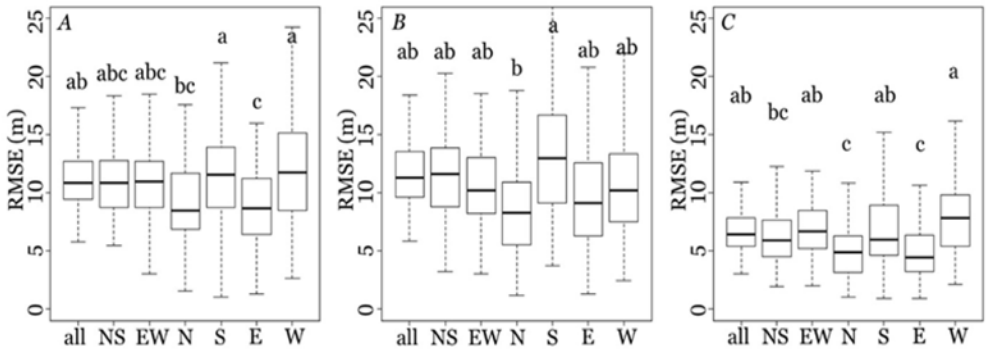

Figure 3: Boxplots for horizontal positional accuracy (RMSE) of observed points using different methods within each GNSS receiver type (A mean center of observed points every cardinal points: all; a mean center of observed points at the North and South: NS; a mean center of observed points at the East and West: EW; a mean center of observed points at the North: N; a mean center of observed points at the South: S; a mean center of observed points at the East: E; a mean center of observed points at the West: W; Garmin Oregon 700: *A*; Suunto GPS watch: *B*; Trimble Juno T41: *C*). *Different letters* indicate significant differences between the groups (p-value <0.05).

and South; East and West), there were no significant differences (Figure 3).

These results suggested that determining a tree bole location using multiple cardinal positions might not be helpful and does not influence horizontal positional accuracy in a forested area. Various factors related to measurement methods have been tested in prior studies to improve the performance of GNSS receivers. For example, Weaver et al. (2015) investigated the effect of holding position for GNSS receivers on horizontal position accuracy and confirmed holding a GNSS receiver vertically provided improved horizontal positional accuracy compared to holding it at an angle or horizontally. Further, Bettinger and Merry (2012a) suggested that the number of fixes to determine the location of tree did not influence horizontal position accuracy, since random trends were observed in different forest types. However, in one case the observation time was considered the most important factor for improving horizontal positional accuracy of GNSS receivers (Næsset & Gjevestad 2008). While our short data collection period may have affected horizontal positional accuracy, the method for collecting positional information in this study represented well the way it is applied in a real-world, practical setting. All this aside, it is interesting to note that due to the difficulties encountered in determining accurate tree positions in a forested environment, it has been suggested that more traditional survey techniques be employed to better represent the true location of individual trees (Edson & Wing 2012). Alternatively, if time and cost were not an issue, the use of survey-grade GNSS receivers or RTK (and other) real-time augmentation methods may better accomplish the mission than using basic mapping-grade or recreation-grade GNSS receivers.

When evaluating the mean center coordinates of the average position determined for each tree using the RSEM, the highest and lowest positional error was also observed when the tree bole locations were determined at single cardinal point (Table 2). The mean center of tree locations determined by each GNSS receiver was located to the South of true tree locations, where the difference from the actual tree bole location had a negative northing regardless of measurement method. Further, most of the mean center X coordinates were biased to the West of the actual tree locations, where the difference from the actual tree location had a negative easting regardless of measurement method and GNSS receiver type. The bias in determined positions was also observed in a previous study using a GPS watch and mapping grade receiver, where the X coordinates were biased to the West of true tree locations regardless of GNSS receiver-grade, season, and forest type, but the reason was not confirmed (Lee et al. 2020). The RSEM values provide a different picture of the horizontal accuracy of the GNSS devices since they somewhat correct for directional error (deviations on two sides of true tree bole positions provide a better estimated representation of the location of trees) while RMSE values ignore directional issues and simply report distance deviation regardless of the direction. For the Garmin receiver, RSEM values ranged from 5–13m, error was often to the South and West of true tree bole positions, the angle of rotation of the estimated ellipse was East-Southeast, and the area of the estimated ellipse was rather large (Table 2). For the Suunto receiver, RSEM values ranged from 5–11m,

Table 2: A summary of the elliptical parameters estimated from positions determined by different GPS equipment using different measurement methods (RSEM = root squared error of the mean; Mean X coordinate = the mean of difference between observed X coordinates and control X coordinate; Mean Y coordinate = the mean of difference between observed Y coordinates and control Y coordinate; I_a = the anisotropic ratio).

Device / metrics	Measurement Methods								
Garmin Oregon 700	All	Two	NS	EW	Single	N	S	E	W
Mean RSEM (m)	7.54	7.54	7.39	7.70	7.54	6.21	9.39	5.62	10.34
Mean X coordinate (m)	-1.45	-1.45	-1.26	-1.65	-1.45	-3.38	0.86	0.82	-4.11
Mean Y coordinate (m)	-7.40	-7.40	-7.28	-7.53	-7.40	-5.21	-9.35	-5.56	-9.49
Angle of rotation (°)	108.57	104.20	106.23	100.65	101.42	100.17	113.60	109.84	59.46
Ia (%)	37.38	30.80	39.50	22.19	21.19	32.10	26.11	33.30	14.27
Area of ellipse (m^2)	110.32	153.92	144.15	160.69	242.97	202.78	207.68	199.62	226.92
Suunto watch GPS	All	Two	NS	EW	Single	N	S	E	W
Mean RSEM (m)	7.85	7.85	7.78	7.94	7.85	5.00	11.00	6.97	9.48
Mean X coordinate (m)	-0.09	-0.09	0.17	-0.35	-0.09	-1.62	1.96	1.84	-2.54
Mean Y coordinate (m)	-7.85	-7.85	-7.78	-7.93	-7.85	-4.74	-10.83	-6.73	-9.13
Angle of rotation (°)	95.92	88.05	95.16	66.30	87.20	107.97	83.87	24.27	61.67
Ia (%)	32.30	24.37	42.00	13.39	13.10	37.31	40.28	13.57	16.17
Area of ellipse (m^2)	127.59	198.80	160.41	225.73	362.79	237.93	300.93	532.02	200.14
Trimble Juno T41	All	Two	NS	EW	Single	N	S	E	W
Mean RSEM (m)	4.55	4.55	4.01	5.09	4.55	3.22	5.21	3.52	6.89
Mean X coordinate (m)	-0.66	-0.66	-0.73	-0.59	-0.66	-1.78	0.32	0.62	-1.79
Mean Y coordinate (m)	-4.50	-4.50	-3.94	-5.06	-4.50	-2.68	-5.20	-3.47	-6.65
Angle of rotation (°)	121.77	134.35	128.96	138.14	148.90	154.33	121.33	168.06	114.41
Ia (%)	21.19	16.71	22.81	9.11	10.81	16.18	24.07	19.58	5.73
Area of ellipse (m^2)	27.78	47.36	50.35	42.07	95.24	79.60	100.10	69.78	81.24

error was often to the South and West of true tree bole positions, the angle of rotation of the estimated ellipse was Northeast-East, and the area of the estimated ellipse was generally larger than that estimated for the Garmin device. For the Trimble receiver, RSEM values ranged from 3–7m, error was often to the South and West of true tree bole positions, the angle of rotation of the estimated ellipse was Southeast, and the area of the estimated ellipse was smaller than that estimated for the other devices. The anisotropic ratios for tree locations determined by the Trimble receiver were lower, indicating it generally had lower bias in direction than the other two devices. In concert with the previously reported results, the mapping-grade receiver provided the most accurate estimates of tree bole positions with the lowest amount of variation.

Regarding the second hypothesis of this study, the ANN analysis of the point pattern of true tree bole locations (control point pattern) suggested it had a dispersed pattern (regular pattern), and that it was significantly different from the CSR (Table 3). The ANN ratio for the control point pattern indicated that it had longer average distance to the nearest tree compared to the expected average distance under CSR (ANN ratio = 1.49). Statistically, observed point patterns from other methods were internally similar when the tree bole locations were measured at two cardinal points (North and South) using the Garmin receiver and when the tree bole locations were determined at two sides (East and West), and South and East using Suunto GPS watch (Table 3). Therefore, we assumed these point patterns might be meaningful to proceed further with spatial point pattern analyses such as $g(r)$ function, $K(r)$ function and $\hat{L}(r)$ function. In addition, we investigated observed point patterns to decide, which point patterns should proceed with further analyses (Figure 4, 5, and 6).

However, most observed patterns seemed to not resemble the control point pattern; thus, we decided to choose the point patterns measured by method "All", which represented lines of trees regardless of GNSS re-

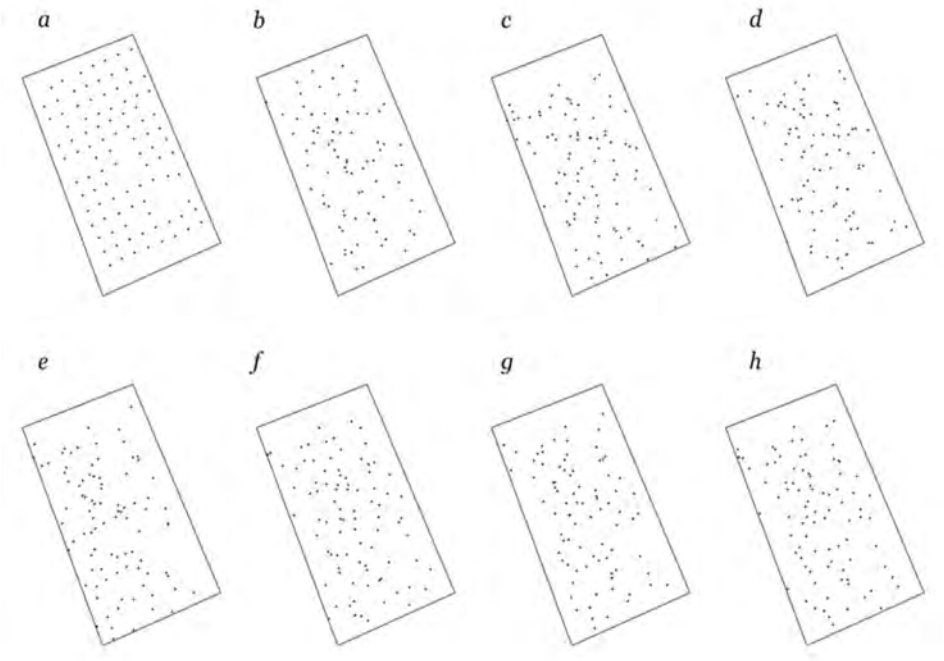

Figure 4: The point patterns observed by Garmin receiver depending on measurement method (a: true location, b: North, c: South, d: East, e: West, f: North and South, g: East and West, h: All).

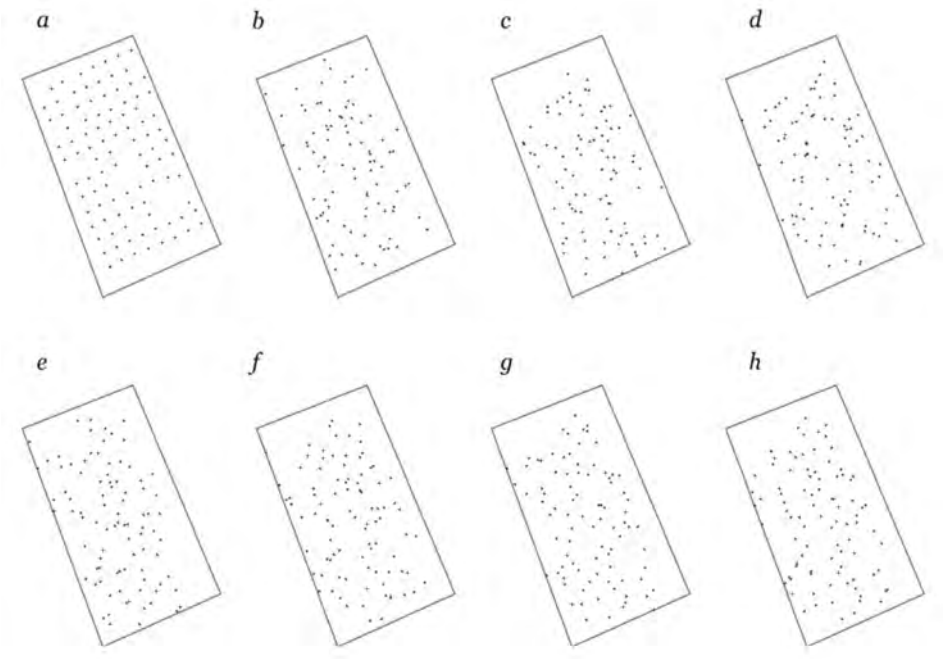

Figure 5: The point patterns observed by the Suunto GPS watch depending on measurement method (a: true location, b: North, c: South, d: East, e: West, f: North and South, g: East and West, h: All).

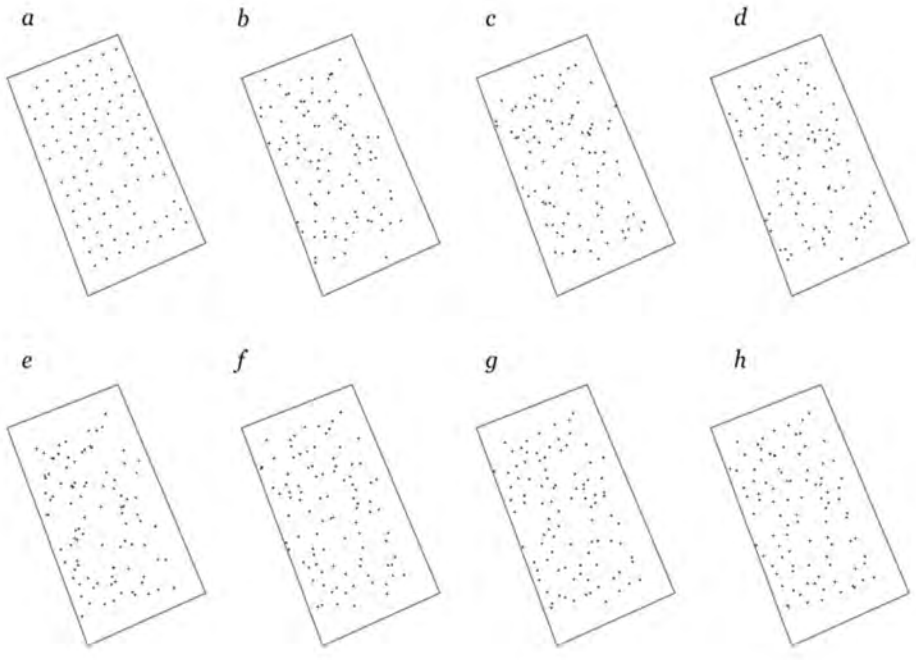

Figure 6: The point patterns observed by the Trimble GNSS receiver depending on measurement method (a: true location, b: North, c: South, d: East, e: West, f: North and South, g: East and West, h: All).

ceiver. Lastly, three observed point patterns by GNSS receiver were selected based on mean RMSE from the smallest value. Therefore, we analyzed point patterns measured by method "NS", "S", and "N" for the Garmin receiver. Regarding the Suunto GPS watch, point patterns observed by method "N", "E", and "W" were selected. The point patterns from the Trimble receiver included points patterns determined by method "NS", "N", and "E". In sum, a total of 15-point patterns including the control point pattern were selected for further spatial analysis such as $g(r)$ function, $K(r)$ function and $\hat{L}(r)$ function.

The control point pattern represented a statistically significant dispersed pattern (regular pattern) at distances of 3 to 7m, which is consistent with the actual average tree spacing of 6.12m (Figure 7, 8, 9 a). At a larger distance scale, there was no evidence of either aggregation or regularity when $K(r)$ and $\hat{L}(r)$ functions were applied (Figure 7, 8 a). Regarding the observed point pattern from using GNSS receivers and methods, the $K(r)$ lines did not represent significant deviation from the expected line, which indicates the point patterns follow complete randomness (Figure 7). However, statistically significant clustered patterns were observed at the wider distance range regardless of GNSS receivers and methods except the point pattern observed by the Garmin receiver using method "E" (Figure 7). The $\hat{L}(r)$ function also detected clustered patterns at larger distance range, but the dispersed pattern (regular pattern) was not observed in any observed point patterns (Figure 8). The $\hat{L}(r)$ function suggested that point patterns observed with the Garmin and Trimble receivers using measurement method "E" followed the complete randomness across distance ranges (Figure 8 j and o). Unlike $K(r)$ and $\hat{L}(r)$ function, the $g(r)$ function detected some evidence of a clustered pattern at certain distances from the control point pattern in addition to the evidence of regularity at the distance scale of around 5m (Figure 9 a). For example, the suggestive evidence of aggregation was confirmed at around 7, 9, 15, and 20m of distance scale. Regarding the observed point patterns, a significant dispersed pattern (regular pattern) was not detected. Rather, $g(r)$ function lines for observed point patterns showed almost no deviation from the expected values indicating a random distribution (Figure 9). In addition, a statistically significant clumpy distribution was observed at various distances regardless of GNSS receiver and method employed. We had assumed that direction of error would be similar with data collected by each device during a short period of time, but this was not necessarily the case (Figure 10).

In sum, each of the basic mapping-grade and recreation-grade GNSS receivers we tested provided a pattern of determined tree bole positions that did not reflect the original pattern of the trees in the seed orchard. In fact, the determined tree positions provided

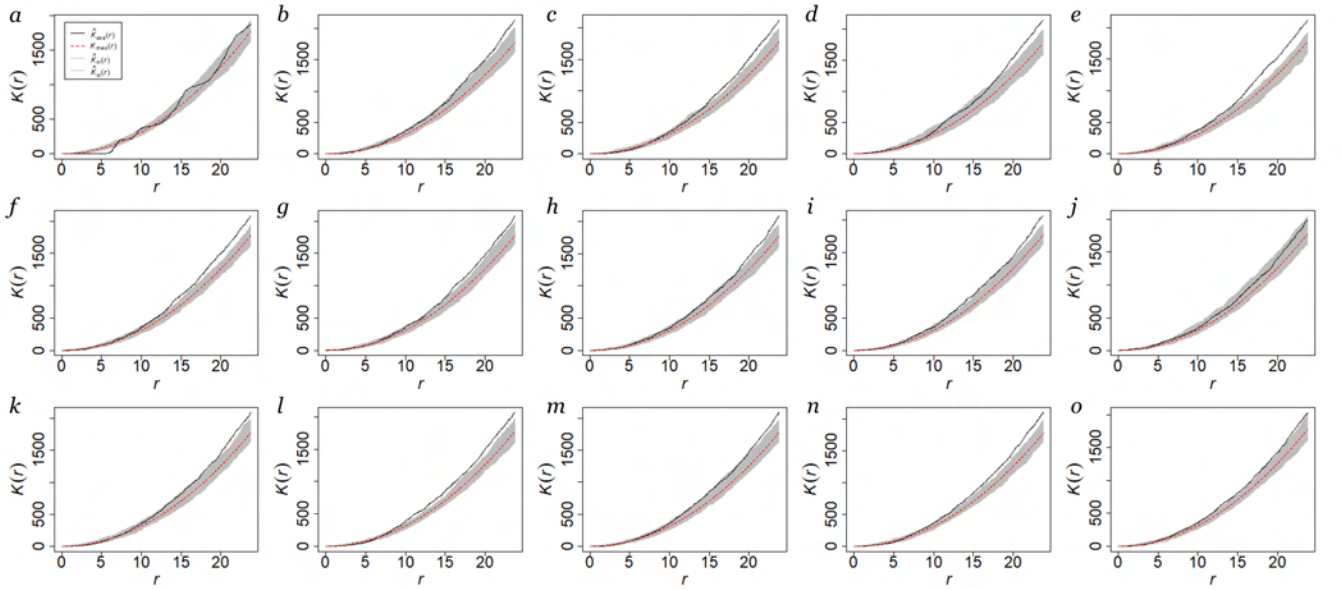

Figure 7: Ripley's K functions ($K(r)$) for point patterns observed by different GNSS receivers and measurement methods (*a*: True tree location; *b, c, d, e*: Garmin receiver; *f, g, h, i, j, k*: Suunto GPS watch; *l, m, n, o*: Trimble receiver; b, f, l: method "All"; c, m: method "NS"; g: method "EW"; d, h, n: method "N"; i: method "S"; e, j, o: method "E"; k: method "W"). Horizontal axes are the distances r between pairs of individuals. Heavy lines show the observed statistic, and the horizontal red dotted lines show the value of $K(r)$ expected from a Poisson process. Gray lines are approximate 95% confidence envelopes for the hypothesis of complete spatial randomness, obtained from 200 independent randomizations of the locations of the trees.

an ANN ratio that was close to 1, reflecting a tendency toward the representation of a random pattern of trees rather than a regular arrangement of trees. Based on the ANN ratio, the pattern of determined tree positions from the Garmin and Suunto devices probably better reflected the original pattern of the tree boles in the seed orchard, yet still did not represent the pattern adequately when applying other summary statistics. Further research in this mission to use GNSS receivers to denote the location of trees in a forested setting seems necessary. If one chooses to accept the mission, it might involve determining whether the use of a RTK GNSS system or other augmentation methods such as DGPS and SLAM can overcome the limitations associated with unaugmented GNSS position fixes collected with autonomous recreation-grade GNSS receivers can develop relatively accurate databases of individual tree bole locations within forests that also maintain the fidelity of the actual tree pattern.

4 Conclusions

In this study, various methods to determine tree bole locations using GNSS receivers were investigated using horizontal positions (point locations) determined by GNSS receivers. In addition, various summary statistics were applied to assess whether the pattern of the control points and the observed points (the GNSS-determined positions) was indeed regular at a distance range, which is equivalent to the average tree spacing (around 6 m) in a pine seed orchard. Given that the range of horizontal position error was greater than the spacing between the real trees, it was not unexpected that the tree bole locations determined by the three GNSS receivers were not representative of the actual regular pattern of tree boles. The results of the spatial point pattern analysis only indicated a significant regular pattern of trees from the very careful field measurement of the control points. These results and ranges of horizontal position error are relevant to other efforts, which use non-augmented GNSS technology in forested areas. These results suggest that even acceptable ranges of horizontal positional error from unaugmented, basic GNSS technology can be associated with a self-destruction of the actual spatial point pattern of trees in a forested setting.

Acknowledgements

We thank the Warnell School of Forestry and Natural Resources at the University of Georgia for supporting this research.

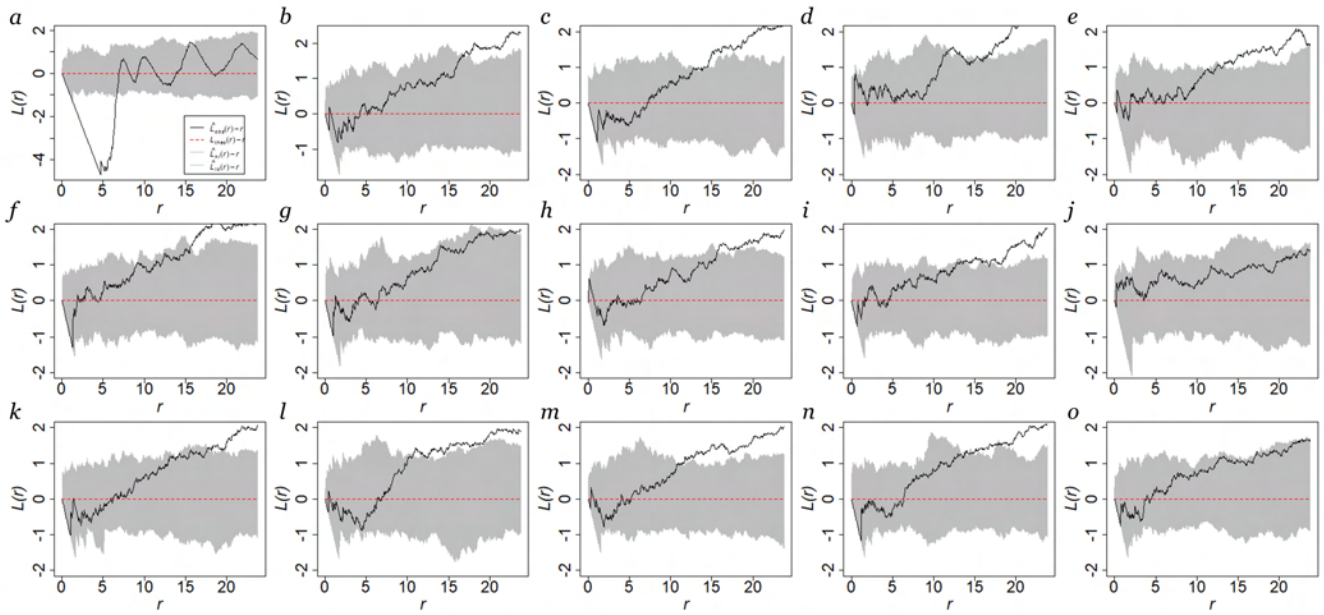

Figure 8: The normalized $L(r)$ functions ($\hat{L}(r)$) for point patterns observed by different GNSS receivers and measurement methods (a: True tree location; b, c, d, e: Garmin receiver; f, g, h, i, j, k: Suunto GPS watch; l, m, n, o: Trimble receiver; b, f, l: method "All"; c, m: method "NS"; g: method "EW"; d, h, n: method "N"; i: method "S"; e, j, o: method "E"; k: method "W"). Horizontal axes are the distances r between pairs of individuals. Heavy lines show the observed statistic, and the horizontal red dotted lines show the value of $\hat{L}(r)$ expected from a Poisson process. Gray lines are approximate 95% confidence envelopes for the hypothesis of complete spatial randomness, obtained from 200 simulations.

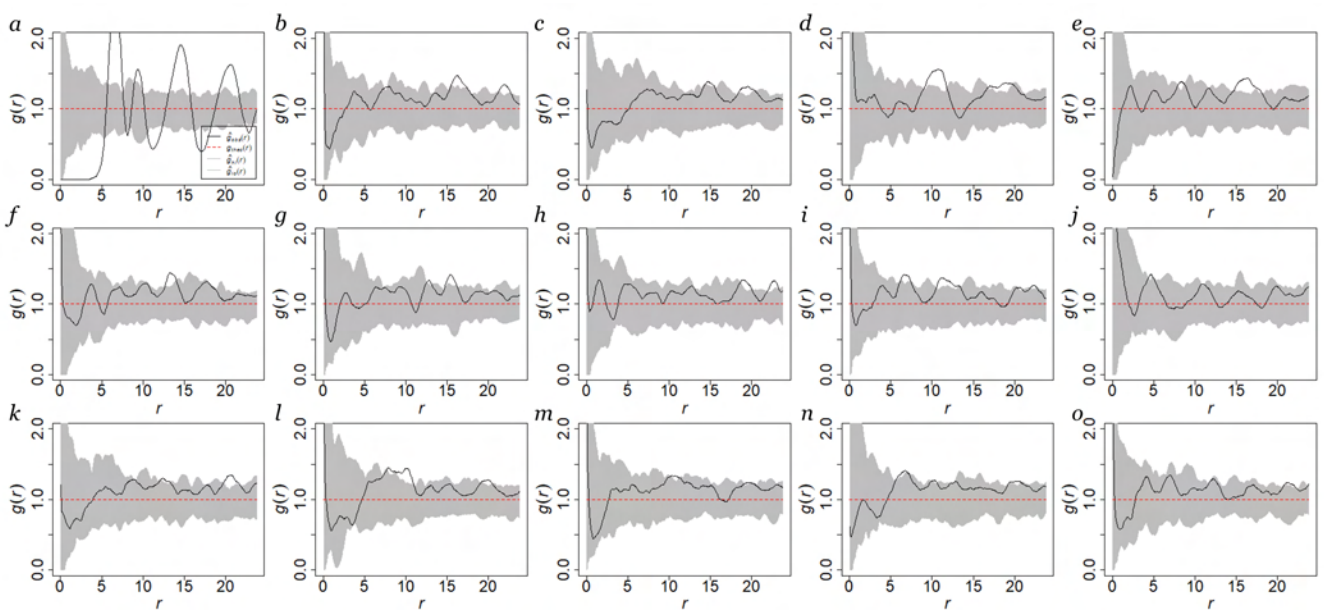

Figure 9: Pair correlation ($g(r)$ function) for point patterns observed by different GNSS receivers and measurement methods (a: True tree location; b, c, d, e: Garmin receiver; f, g, h, i, j, k: Suunto GPS watch; l, m, n, o: Trimble receiver; b, f, l: method "All"; c, m: method "NS"; g: method "EW"; d, h, n: method "N"; i: method "S"; e, j, o: method "E"; k: method "W"). Horizontal axes are the distances r between pairs of individuals. Heavy lines show the observed statistic, and the horizontal red dotted lines show the pair correlation function expected from a Poisson process. Gray lines are 95% Monte Carlo simulation envelopes obtained from 200 simulations.

Table 3: A summary of average nearest neighbor (ANN) analysis for different GNSS receivers and measurement methods.

True tree location	1.49	9.82	<0.01
Measur. method	ANN ratio	z-score	p-value
	Garmin Oregon 700		
All	1.09	1.69	0.09
NS	1.16	3.01	<0.01
EW	1.10	1.79	0.07
N	1.06	1.14	0.25
S	1.03	0.53	0.59
E	1.04	0.81	0.42
W	1.12	2.28	0.02
	Suunto GPS Watch		
All	1.05	0.98	0.33
NS	1.02	0.45	0.65
EW	1.20	3.80	<0.01
N	1.01	0.26	0.79
S	1.16	2.93	<0.01
E	1.20	3.81	<0.01
W	1.12	2.19	0.03
	Trimble Juno T41		
All	1.03	0.5	0.62
NS	0.98	-0.32	0.75
EW	1.08	1.55	0.12
N	1.03	0.53	0.60
S	0.95	-0.92	0.36
E	1.05	0.97	0.33
W	0.90	-1.96	0.05

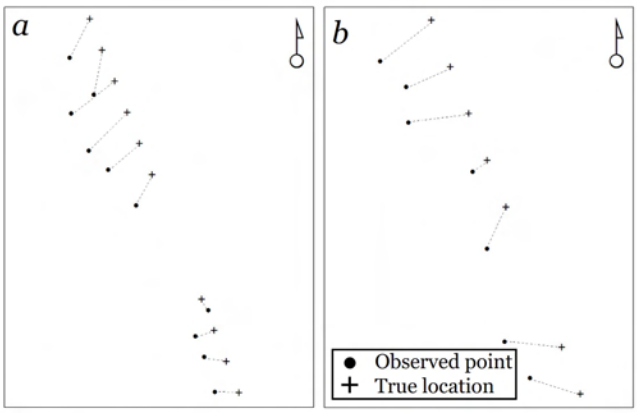

Figure 10: The direction of error for data collected by Trimble receiver using "All" method within short period of time (a: collected on February 22^{nd}, 2021; b: collected on March 6^{th}, 2021).

References

Aguirre, O., Hui, G., Gadow, K.v. and Jiménez, J., 2003. An analysis of spatial forest structure using neighbourhood-based variables. Forest Ecology and Management, 183, 137–145.

Atkinson, P.M., Foody, G.M., Gething, P.W., Mathur, A. and Kelly, C.K., 2007. Investigating spatial structure in specific tree species in ancient semi-natural woodland using remote sensing and marked point pattern analysis. Ecography, 30(1), 88–104.

Besag, J., 1977. Contribution to the discussion on Dr. Ripley's paper. Journal of the Royal Statistical Society, Series B, 39, 93–195.

Bettinger, P. and Fei, S., 2010. One year's experience with a recreation-grade GPS receiver. Mathematical and Computational Forestry & Natural-Resource Sciences, 2(2), 153–160. Retrieved from `http://mcfns.net/index.php/Journal/article/view/MCFNS.2-153` on Apr. 30, 2022.

Bettinger, P. and Merry, K., 2012a. Static horizontal positions determined with a consumer-grade GNSS receiver: One assessment of the number of fixes necessary. Croatian Journal of Forest Engineering, 33(1), 149–157.

Bettinger, P. and Merry, K.L., 2011. Global navigation satellite system research in forest management: A summary of horizontal, vertical, static, and dynamic accuracy assessments. LAP Lambert Academic Publishing, Saarbrücken, Germany. 64 p.

Bettinger, P. and Merry, K.L., 2012b. Influence of the juxtaposition of trees on consumer-grade GPS position quality. Mathematical and Computational Forestry & Natural-Resource Sciences, 4(2), 81–91. Retrieved from `http://mcfns.net/index.php/Journal/article/view/140` on Apr. 30, 2022.

Bettinger, P., Merry, K., Bayat, M. and Tomaštík, J. 2019. GNSS use in forestry—A multi-national survey from Iran, Slovakia and southern USA. Computers and Electronics in Agriculture, 158, 369–383.

Carrer, M., Castagneri, D., Popa, I., Pividori, M. and Lingua, E., 2018. Tree spatial patterns and stand attributes in temperate forests: The importance of plot size, sampling design, and null model. Forest Ecology and Management, 407, 125–134.

Clark, P.J. and Evans, F.C., 1954. Distance to nearest neighbor as a measure of spatial relationships in populations. Ecology, 35(3), 445–453.

Danskin, S.D., Bettinger, P., Jordan, T.R. and Cieszewski, C., 2009. A comparison of GPS performance in a southern hardwood forest: Exploring low-cost solutions for forestry applications. Southern Journal of Applied Forestry, 33(1), 9–16.

Diggle, P.J., 2013. Statistical analysis of spatial and spatio-temporal point patterns. Monographs on Statistics and Applied Probability 128. CRC Press, Boca Raton, FL.

Dohn, J., Augustine, D.J., Hanan, N.P., Ratnam, J. and Sankaran, M., 2017. Spatial vegetation patterns and neighborhood competition among woody plants in an East African savanna. Ecology, 98(2), 478–488.

Edson, C. and Wing, M.G., 2012. Tree location measurement accuracy with a mapping-grade GPS receiver under forest canopy. Forest Science, 58(5), 567–576.

Fajardo, A., Goodburn, J.M. and Graham, J., 2006. Spatial patterns of regeneration in managed uneven-aged ponderosa pine/Douglas-fir forests of western Montana, USA. Forest Ecology and Management, 223, 255–266.

Fan, Y., Feng, Z., Mannan, A., Khan, T.U., Shen, C. and Saeed, S., 2018. Estimating tree position, diameter at breast height, and tree height in real-time using a mobile phone with RGB-D SLAM. Remote Sensing, 10(11), Article 1845.

Fauzi, M.F., Idris, N.H., Din, A.H.M., Osman, M.J. and Ishak, M.H.I., 2016a. Indiginous community tree inventory: Assessment of data quality. The International Archives of the Photogrammetry, Remote Sensing and Spatial Information Sciences, 42(3), 307–314.

Fauzi, M., Idris, N., Yahya, M., Din, A., Lau, A. and Ishak, M. 2016b. Tropical forest tree positioning accuracy: A comparison of low cost GNSS-enabled devices. International Journal of Geoinformatics, 12(2), 59–66.

Gadow, K.v. and Hui, G.Y., 2002. Characterizing forest spatial structure and diversity. In Sustainable Forestry in Temperate Regions, Björk, L. (ed.). SUFOR, University of Lund, Lund, Sweden, pp. 20–30.

Gadow, K.v., Zhang, C.Y., Wehenkel, C., Pommerening, A., Corral-Rivas, J., Korol, M., Myklush, S., Hui, G.Y., Kiviste, A. and Zhao, X.H., 2012. Forest structure and diversity. In Continuous cover forestry. pp. 29–83. Springer, Dordrecht, The Netherlands.

Garzon-Lopez, C.X., Jansen, P.A., Bohlman, S.A., Ordonez, A. and Olff, H., 2014. Effects of sampling scale on patterns of habitat association in tropical trees. Journal of Vegetation Science, 25(2), 349–362.

Green, L.Y., Mikhailova, E.A., Post, C.J., Darnault, C.C.J.G., Bridges, W.C. and Schlautman, M.A., 2016. A cloud-based spatial-temporal inventory for sustainable urban soil management. Urban Ecosystems, 19(2), 811–822.

Hui, G., Li, L., Zhao, Z. and Dang, P., 2007. Comparison of methods in analysis of the tree spatial distribution pattern. Acta Ecologica Sinica, 27(11), 4717–4728.

Hung, I., Unger, D., Kulhavy, D. and Zhang, Y., 2019. Positional precision analysis of orthomosaics derived from drone captured aerial imagery. Drones, 3(2), Article 46.

Illian, J., Penttinen, A., Stoyan, H. and Stoyan, D., 2008. Statistical analysis and modelling of spatial point patterns. John Wiley & Sons Ltd., West Sussex, England.

Khot, L.R., Tang, L., Blackmore, S.B. and Nørremark, M., 2006. Navigational context recognition for an automomous robot in a simulated tree plantation. Transactions of the ASABE, 49(4), 1579–1588.

Kiser, J., 2008. Chapter 1, Surveying. In Part 650, Engineering field handbook. U.S. Department of Agriculture, Natural Resources Conservation Service, Washington, D.C.

Law, R., Illian, J., Burslem, D.F., Gratzer, G., Gunatilleke, C.V.S. and Gunatilleke, I.A.U.N., 2009. Ecological information from spatial patterns of plants: insights from point process theory. Journal of Ecology, 97(3), 616–628.

Lee, T., Bettinger, P., Cieszewski, C.J. and Gutierrez Garzon, A.R., 2020. The applicability of recreation-grade GNSS receiver (GPS watch, Suunto Ambit Peak 3) in a forested and an open area compared to a mapping-grade receiver (Trimble Juno T41). PLoS ONE, 15(3), e0231532.

Lewis, J.S., Rachlow, J.L., Garton, E.O. and Vierling, L.A., 2007. Effects of habitat on GPS collar performance: using data screening to reduce location error. Journal of Applied Ecology, 44(3), 663–671.

Merry, K., and Bettinger, P. 2019. Smartphone GPS accuracy study in an urban environment. PLoS ONE, 14(6): e0219890.

Moustakas, A., Wiegand, K., Getzin, S., Ward, D., Meyer, K.M., Guenther, M. and Mueller, K.H. 2008. Spacing patterns of an *Acacia* tree in the Kalahari over a 61-year period: How clumped becomes regular and *vice versa*. Acta Oecologica, 33(3), 355–364.

Næsset, E. and Gjevestad, J.G., 2008. Performance of GPS precise point positioning under conifer forest canopies. Photogrammetric Engineering & Remote Sensing, 74(4), 661–668.

Perry, G.L., Miller, B.P. and Enright, N.J., 2006. A comparison of methods for the statistical analysis of spatial point patterns in plant ecology. Plant Ecology, 187(1), 59–82.

Pommerening, A., 2002. Approaches to quantifying forest structures. Forestry, 75(3), 305–324.

Pommerening, A., 2008. Analysing and modelling spatial woodland structure. Bangor University, Wales, UK (DSc dissertation), University of Natural Resources and Applied Life Sciences, Vienna, Austria.

Pommerening, A. and Grabarnik, P., 2019. Individual-based methods in forest ecology and management. Springer Nature Switzerland, Cham.

Ransom, M.D., Rhynold, J. and Bettinger, P., 2010. Performance of mapping-grade GPS receivers in southeastern forest conditions. RURALS: Review of Undergraduate Research in Agricultural and Life Sciences, 5(1), Article 2.

Ripley, B., 1981. Spatial statistics. John Wiley & Sons, Inc., New York.

Seidler, T.G. and Plotkin, J.B., 2006. Seed dispersal and spatial pattern in tropical trees. PLoS Biology, 4(11), e344.

Sigrist, P., Coppin, P. and Hermy, M., 1999. Impact of forest canopy on quality and accuracy of GPS measurements. International Journal of Remote Sensing, 20(18), 3595–3610.

Stoyan, D. and Stoyan, H., 1996. Estimating pair correlation functions of planar cluster processes. Biometrical Journal, 38(3), 259–271.

Tait, R.J., Allen, T.J., Sherkat, N. and Bellett-Travers, M.D., 2009. An electronic tree inventory for arboriculture management. Knowledge-Based Systems, 22(6), 552–556.

Trochta, J., Král, K., Janík, D. and Adam, D., 2013. Arrangement of terrestrial laser scanner positions for area-wide stem mapping of natural forests. Canadian Journal of Forest Research, 43(999), 355–363.

Uria-Diez, J. and Pommerening, A., 2017. Crown plasticity in Scots pine (*Pinus sylvestris* L.) as a strategy of adaptation to competition and environmental factors. Ecological Modelling, 356, 117–126.

Vacchiano, G., Castagneri, D., Meloni, F., Lingua, E. and Motta, R., 2011. Point pattern analysis of crown-to-crown interactions in mountain forests. Procedia Environmental Sciences, 7, 269–274.

Velázquez, E., Martínez, I., Getzin, S., Moloney, K.A. and Wiegand, T., 2016. An evaluation of the state of spatial point pattern analysis in ecology. Ecography, 39(11), 1042–1055.

Weaver, S.A., Ucar, Z., Bettinger, P. and Merry, K., 2015. How a GNSS receiver is held may affect static horizontal position accuracy. PLoS ONE, 10(3), e0124696.

Wiegand, T., He, F. and Hubbell, S.P., 2013. A systematic comparison of summary characteristics for quantifying point patterns in ecology. Ecography, 36(1), 92–103.

Wiegand, T. and Moloney, K.A., 2013. Handbook of spatial point-pattern analysis in ecology. CRC Press, Boca Raton, FL.

Woodall, C., 2002. Point pattern analysis of FIA data. In Proceedings of the Third Annual Forest Inventory and Analysis Symposium, McRoberts, R.E., Reams, G.A., Van Deusen, P.C. and Moser, J.W., (eds.). U.S. Department of Agriculture, Forest Service, North Central Research Station, St. Paul, MN. General Technical Report NC-230. pp. 162–170.

Xu, J., Gu, H., Meng, Q., Cheng, J., Liu, Y., Sheng, J., Deng, J. and Bai, X., 2019. Spatial pattern analysis of *Haloxylon ammodendron* using UAV imagery-A case study in the Gurbantunggut Desert. International Journal of Applied Earth Observation and Geoinformation, 83, Article 101891.